CHARACTERIZATION OF THE LONGITUDINAL ACCEPTANCE IN A STORAGE RING WITH RF PINGER*

G-M. Wang [†], T. Shaftan, J. Rose, Y. Li, B. Holub

Brookhaven National Laboratory, Upton, NY

Abstract

In modern generation light sources, it is desired to have long beam lifetime, which is limited by Touschek scattering. Touschek scattering strongly depends on momentum aperture. Understanding momentum aperture is extremely important. NSLS II storage ring RF system has the digital ramp control function, enabling rapid change of the cavity phase and amplitude. This makes the possibility to "ping" the beam in longitudinal phase space and directly measure the momentum aperture, in contrast with traditional indirect way to understand it from other aspect of parameters. In this paper, we present the tool, 'RF pinger', its application to characterize NSLS II longitudinal acceptance and localize the SR aperture limit with BPM signal.

INTRODUCTION

Modern generation synchrotron light sources have storage ring performance at high beam current, low horizontal emittance with small coupling to vertical plane, resulting in intense Touschek scattering, which is the dominant limitation of beam lifetime [1]. Touschek lifetime, $\frac{1}{\tau} = \frac{r_e^2 c N_0}{8\pi\gamma^3\sigma_z}\frac{1}{C}\oint\frac{F\left(\left[\frac{\delta_{acc}}{\gamma\sigma_{x'}}\right]^2\right)}{\sigma_x\sigma_{x'}\sigma_y\delta_{acc}^2}ds$, depends on the beam parameters, i.e. beam size, divergence, bunch length, single bunch current and SR momentum aperture. There are different strategies to manipulate beam parameters to increase Touschek lifetime. The measured momentum aperture in the existing light sources and colliders showed smaller than the designed values. It is important to characterize SR momentum aperture.

The common way to measure momentum aperture is to fit it from beam lifetime measurement [2-3]. In this paper, we directly measure the momentum aperture in NSLS-II with RF pinger.

NSLS-II is a 3 GeV, synchrotron light source at Brookhaven National Laboratory and started beamline routine operation from 2015 [4]. In Table 1 we list the main parameters in storage ring.

In the following section, we described NSLS-II RF pinger for phase and amplitude jump. We also showed data processing to precisely retrieve longitudinal beam parameters, turn by turn energy oscillation. The experiments were designed with different lattice setting, without and with damping wiggler. From BPMs turn by turn sum signal, we found the SR aperture limitation region.

Table 1: NSLS-II SR Main Parameters

Parameter	Description	Value
E_0	Beam energy	3 GeV
C	Circumference	791.958 m
f_{RF}	RF frequency	500 MHz
V_{RF}	RF voltage	upto 4.9 MV
I_b	Beam current	~3 mA over 40 bunches
ε_x	Horizontal emittance (w/o DWs)	1/2 nm-rad
$\kappa = \varepsilon_y/\varepsilon_x$	Emittance ratio	~0.8%
ν_x	Horizontal tune	33.22
ν_y	Vertical tune	16.26
$\xi 1_x$	Horizontal 1st order chromaticity	2
$\xi 1_y$	Vertical 1st order chromaticity	2
$\eta 1_x$	1st order dispersion	0.42 m
$\eta 2_x$	2nd order dispersion	4 m
K_p	RF proportional gain	0.02
K_i	RF integral gain	0.05

RF PINGER

The NSLS-II storage ring RF system [5] was designed with four 500 MHz superconducting RF (SRF) cavities for replenishing the synchrotron losses of the stored electron beam and two 1500 MHz superconducting RF cavities to increase the Touschek lifetime by lengthening electron bunches. RF cavities were installed in different stage and only two main RF cavities were in operation upto now.

SRF cavities are driven independently by a 300 kW klystron transmitters, with a low level RF drive and feedback that was provided by a digital cavity field controller. The controller provides robust RF feedback with an overall loop delay of 1.1 microseconds. It also provides closed loop and open loop system excitations for a variety of beam and system studies.

A schematic of cavity field controller is shown in Fig. 1. The cavity field controller can operate in open loop feedforward (FF) mode, closed loop feedback (FB) mode or closed loop with either FF table or Network Analyzer functions enabled.

In addition, there is a mode to switch between feedback set points, called a phase jump mode, although the jump is actually in I/Q set points and so can either be an amplitude jump, phase jump or combination.

LLRF controller [6] was modified by adding required controls and external on-demand timing trigger to control the jump event. Once the event is triggered, RF circular buffer is frozen to capture data both before and after the

trigger event. It includes 8 channels' RF cavity signal and 2 channels' beam signals for diagnostic and monitor purpose with 1.7 Mega bites waveform length at 4 MHz sampling rate data acquisition.
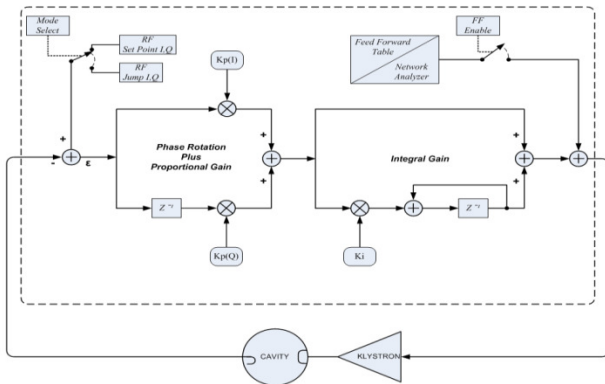

Figure 1: Schematic of NSLS-II cavity field controller.

The RF pinger timing was aligned with other timing driven subsystems, such as transverse pinger, BPMs. The timing delay for the RF pinger trigger was aligned with BPM sum signal so that RF pinger trigger is delayed by 100 turns relative to SR BPMs to monitor beam synchrotron motion at any dispersive BPM. Transverse pingers were also aligned to BPMs. Thus the pingers in all three planes of the beam motion can be excited independently or simultaneously in any combination.

The phase jump has been used in beam dynamics studies [7]. The limiting factors for the magnitude of the phase jump are the forward and reverse power limits of the RF system. These are in turn influenced by the value of the phase jump (180 degrees gives maximum power requirement) and the speed to complete the jump in cavity fields. The jump speed depends on the parameters of feedback gain. When the phase jump is triggered the set points immediately change to new values. The cavity field fed into the controller is subtracted from this set point and the error is multiplied by the feedback gains to drive the system to the new values. RF gain parameters K_p and K_i were optimized to maximize longitudinal oscillation.

DATA PROCESSING TECHNIQUES

Beam energy oscillation δ from RF phase jump is measured with BPMs located in dispersive region (from the optics model the dispersion is 0.42 m of η_1 and -3 m of η_2). When δ is in the range of 2%, the beam position oscillates to the extent of 10 mm and the contributions from the second order dispersion cannot be ignored.

With large beam offsets, BPM position 5th order correction is needed:

$$x_{corr} = p_{10}\left(\frac{\Delta}{\Sigma}\right)_x + p_{30}\left(\frac{\Delta}{\Sigma}\right)_x^3 + p_{50}\left(\frac{\Delta}{\Sigma}\right)_x^5$$

Here p_{10}, p_{30}, p_{50} are the BPM coefficient from model calibration, depending on the BPM design. $\frac{\Delta}{\Sigma}$ is the button signal combination.

Figure 2 showed an example of dispersion BPM TBT data without and with high order calibration. RF phase

jump excites beam synchrotron oscillation. At small phase jump, the oscillation amplitude is symmetry and non-linearity is small. At large phase jump, the beam position reading is asymmetric. One contribution is from BPM non-linearity and the other factor is from second order dispersion contribution.
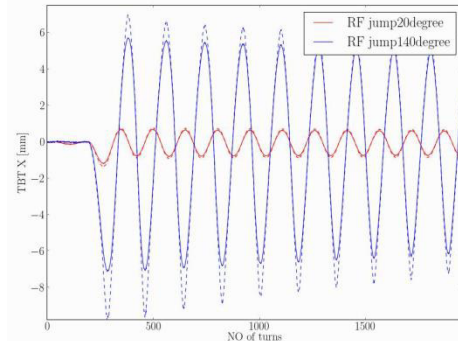

Figure 2: BPMs TBT data non-linear calibration.

In addition, the beam position depends on δ as $x = \eta_1 * \delta + \eta_2 * \delta^2$. The energy oscillation written in terms of position is:

$$\delta = \frac{2x}{\left(\eta_1 + \sqrt{\eta_1^2 + 4\eta_2 x}\right)}$$

This solution is convenient for using in both linear and linear and 2nd order dispersion cases.

With the above 2-step data processing, the TBT beam energy oscillation can be retrieved from BPM TBT position.

EXPERIMENTS

Momentum aperture is limited by either physical aperture or dynamic aperture or RF momentum aperture. NSLS-II physical aperture is larger than the other two limitations. With RF cavities voltage in full operation value, its momentum aperture is designed as >2.6%, ultimately limited by the dynamic aperture.

In this study, SR RF cavity was operated at 1.77 MV. NSLS-II has three damping wigglers and they impact the energy loss dramatically while changing the gap status between open and close, thus changes the momentum aperture under the same RF voltage. The energy loss per turn with damping wiggler open is 286 keV and the value increases to 700 keV with three DWs gaps closed. In the experiment, we studied two cases, by changing the status of DWs and vary the RF bucket height at 2.4% and 1.8% respectively. Notice that in both cases, the RF momentum aperture is the same as RF bucket height, which was confirmed in beam lifetime measurement [8]. It is smaller than dynamic or physical apertures.

We increased the RF phase jump amplitude gradually until the beam energy oscillation reaches momentum aperture limit and beam was lost. Figure 3 shows the process of beam longitudinal phase space turn by turn evolution with different phase jump. The horizontal axis is beam phase oscillation relative to the synchrotron phase, reading from RF system data and vertical axis is beam energy offset, retrieved from BPM turn by turn data. With RF phase jump amplitude increase, the phase

space gradually distorted from elliptical shape until the beam is out of stable region.
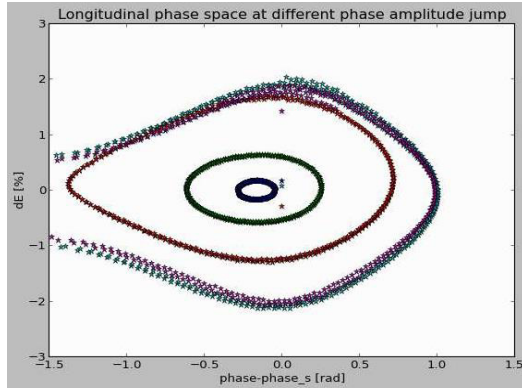

Figure 3: beam longitudinal phase space at different RF phase jump amplitude.

Figure 4 showed the result of momentum aperture edge, where the beam starts to lose. It includes two cases, with damping wiggler open (blue trace) and close (red trace). The solid curve is for RF phase jump amplitude in left axis and the dashed curve is beam intensity at different turns from BPM TBT sum signal. SR BPMs TBT positions in horizontal plane are used to measure the actual beam energy oscillation. The results showed that without DW, beam loses with phase jump at 150 degree with measured δ_{max} at 2.4%. With DWs, we lost beam with phase jump at 120 degree and the measured δ_{max} is 1.8%. This agrees with expectation that the momentum aperture is limited by RF bucket height and it is smaller with DWclose than open state.
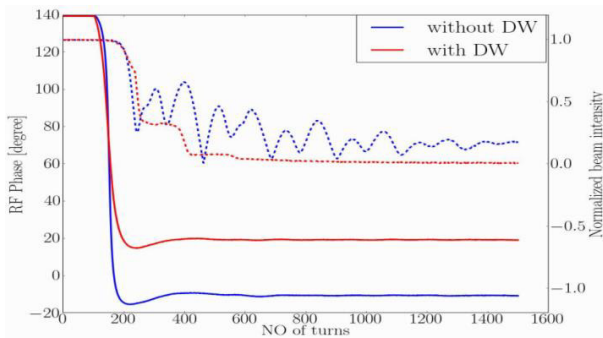

Figure 4: RF momentum aperture measurement without and with DW.

In the experiment, we also increased RF total voltage further so that RF bucket height is larger than designed momentum aperture and machine is limited by dynamic aperture. This required beam energy excitation larger than 2.6%. It turns out that RF transmitter trips from high reflection power and limits the maximum energy oscillation. To reach the aperture limit set by the dynamic aperture, we shifted RF frequency statically to set the beam off-momentum in addition to the RF jump.

The results are shown in Fig. 5. The left plot shows one BPM TBT intensity and beam position X oscillation. As predicted, the beam loss only happens in one side of the energy oscillations with synchrotron period. To find out where the dynamic aperture limit locates in the ring, we firstly zoom in a small region corresponding to beam loss

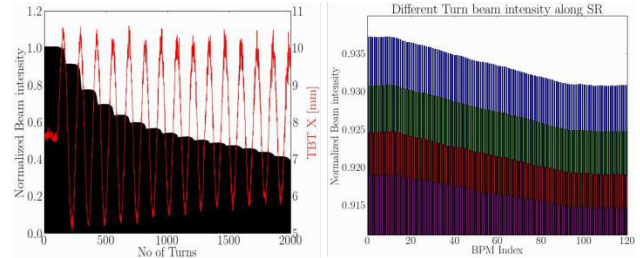and then selected this region of a few turns from all 180 BPMs for analysis.

Figure 5: dynamic aperture limit location.

The BPM sum signal exhibited level of noise in excess of slow loss rate due to the RF jump. Even with the normalized sum data BPM-to-BPM noise is still comparable with the beam loss in one turn and it is hard to judge where the beam is actually lost. To reduce the noise, the raw data was further processed by moving data average method. First, 180 BPMs different turns data was expanded into a long transport line in BPM sequence and turn sequence, as: $I_{raw} = [I_i^{p1}, ..., I_i^{pn}, I_{i+1}^{p1} ...]$, where pn is the BPM index number and i is the turn number. Then beam sum signal was processed via moving average as $\overline{I_i^{pj}} = mean(I_i^{pj}, ... I_i^{pj+k})$, where k is the slice number of averaged BPMs. The beam loss locations (Fig. 5) are pointed by sudden slope changes in the sum signal. The data points to the location of EPU ID in cell 23 of NSLS-II ring. This is consistent with radiation dose measurement result.

SUMMARY AND OUTLOOK

High precision RF pinger system was commissioned and implemented at NSLS-II. This tool enables various beam dynamics studies that require transient excitation of synchrotron oscillations.

With RF pinger, we directly measured the NSLS-II momentum aperture at different lattice set, without and with damping wiggler. The result agrees with the prediction that at low voltage, the momentum aperture is limited RF bucket height. Under the limitation of RF reflection power, we pin-pointed the dynamic aperture location by shifting the beam off-energy statically in addition to the RF jump.

ACKNOWLEDGMENT

REFERENCES

[1] B. Podobedov, et.al, IPAC2015, MOPJE053.

[2] C. Steier, Phys. Rev. E 65, 056506.

[3] B. Nash, et. al, IPAC2011, THPC008.

[4] T. Shaftan, IPAC2016, WEPOY05.

[5] J. Rose, et.al, PAC2011, FROBS4

[6] B. Holub, et.al, IPAC2015, MOPTY038.

[7] G-M Wang, et. al, IPAC2016, THOBA01.

[8] G-M Wang, T. Shaftan, et.al, Rev. Sci. Instrum. 87, 033301 (2016).